

Nanometer-accurate Grating Fabrication with Scanning Beam Interference Lithography

Carl G. Chen, Paul T. Konkola, Ralf K. Heilmann, Chulmin Joo, and Mark L. Schattenburg
Space Nanotechnology Laboratory, Massachusetts Institute of Technology,
Cambridge, MA 02139, USA

ABSTRACT

We are developing a Scanning Beam Interference Lithography (SBIL) system. SBIL represents a new paradigm in semiconductor metrology, capable of patterning large-area linear gratings and grids with nanometer overall phase accuracy. Realizing our accuracy goal is a major challenge because the interference fringes have to be locked to a moving substrate with nanometer spatial phase errors while the period of the fringes has to be stabilized to approximately one part per million. In this paper, we present a review of the SBIL design, and report recent progress towards prototyping the first-ever SBIL tool.

Keywords: Scanning Beam Interference Lithography, SBIL, Interference Lithography, Grating, Metrology, Displacement Measuring Interferometry, Fringe Locking, Phase Shifting Interferometry

1. INTRODUCTION

In using “traditional” interference lithography (IL)¹ to pattern a grating, one splits a laser beam in two and spatially filters them to produce two spherical waves. The waves interfere and the resulting fringes are recorded in photoresist. The nominal grating period, p , is given by

$$p = \frac{\lambda}{2 \sin \theta}, \quad (1)$$

where λ is the wavelength of the laser, and θ is the incident angle of the waves. The interference of two coherent laser beams ensures that the grating has high phase coherence. Its phase progression, however, is inherently hyperbolic due to the spherical wavefront curvature.¹⁻⁴ It is questionable as to whether one can apply traditional IL to pattern large-area gratings that have close-to-ideal linear phase.⁵

By interfering two small-diameter laser beams and step-and-scanning the resulting grating patch, Scanning Beam Interference Lithography (SBIL)⁵⁻⁷ is designed to pattern large-area linear gratings and grids with nanometer, and ultimately, subnanometer overall phase distortions. Figure 1 depicts the SBIL concept. Our tool operates with a CW argon-ion laser ($\lambda = 351.1$ nm) and can pattern gratings on photoresist-covered substrates that are up to 300 mm in diameter.

SBIL represents a new paradigm in semiconductor metrology.^{6,8} Linear gratings and grids patterned by SBIL can serve as metrology standards, and can be used to solve a variety of critical metrology problems that have become increasingly difficult to tackle with present-day technologies. In addition, they may also enable important advances in fields such as microphotonics, nanomagnetism, optical encoding and high-resolution spectroscopy.

Realizing nanometer-level SBIL performance is a major challenge, because the interference fringes have to be locked to a moving substrate with nanometer spatial phase errors, while the period of the fringes has to be stabilized to approximately one part per million. Many error sources exist, which can be classified into five categories: displacement measuring interferometer, lithography interferometer, substrate and metrology frame, period control and beam alignment, and Gaussian wavefront errors.

We review how our design brings these error categories under control. We regard each one of these categories a major SBIL subsystem, and address them in sequence.

Further author information: (Send correspondence to C.G.C.)
C.G.C.: E-mail: gangchen@mit.edu

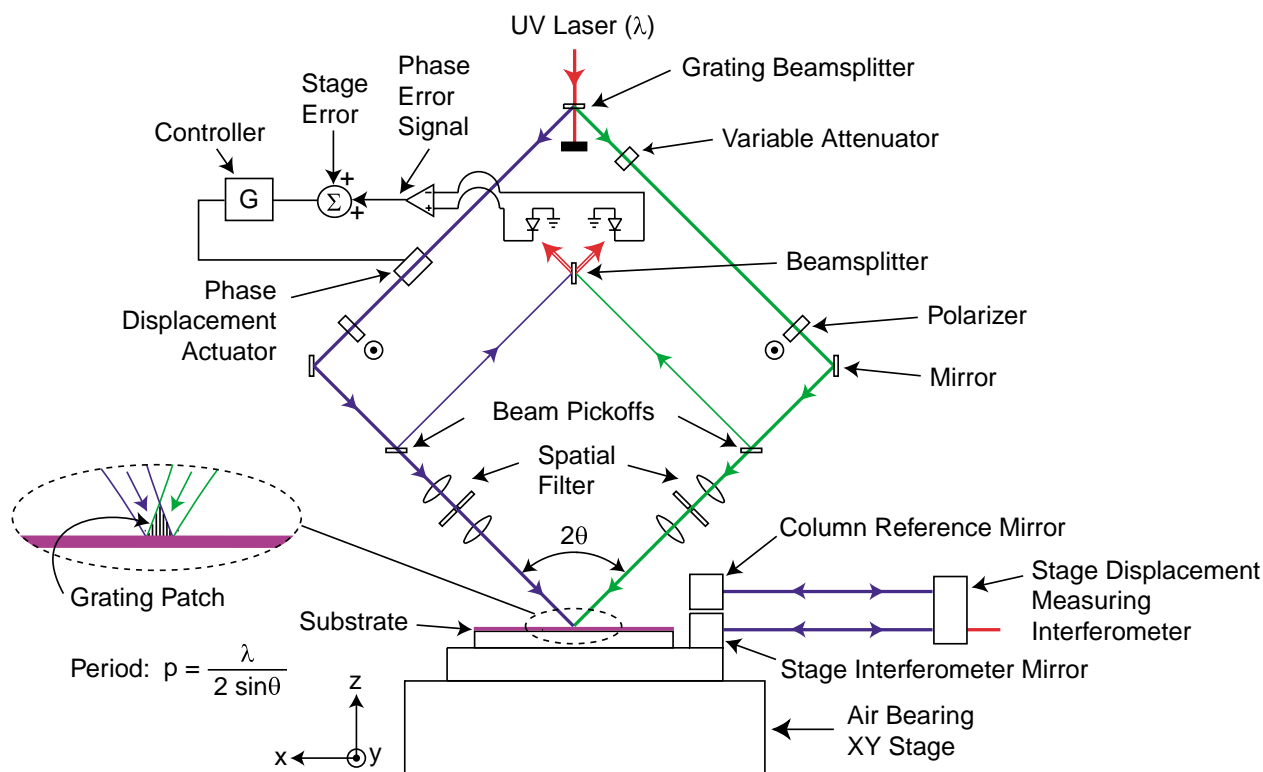


Figure 1. SBIL optics closely resemble those of traditional IL but the interference image is much smaller than the total desired patterning area. Large gratings are fabricated by step-and-scanning the substrate underneath a small grating patch. Typically, the patch has a diameter between $200\ \mu\text{m}$ and $2\ \text{mm}$. In our tool, prior to writing, the grating period can be set to any desired value between $200\ \text{nm}$ and $2\ \mu\text{m}$. A fringe-locking controller locks the interference image to the moving substrate by correcting for the stage error and the lithography interferometer's phase error.

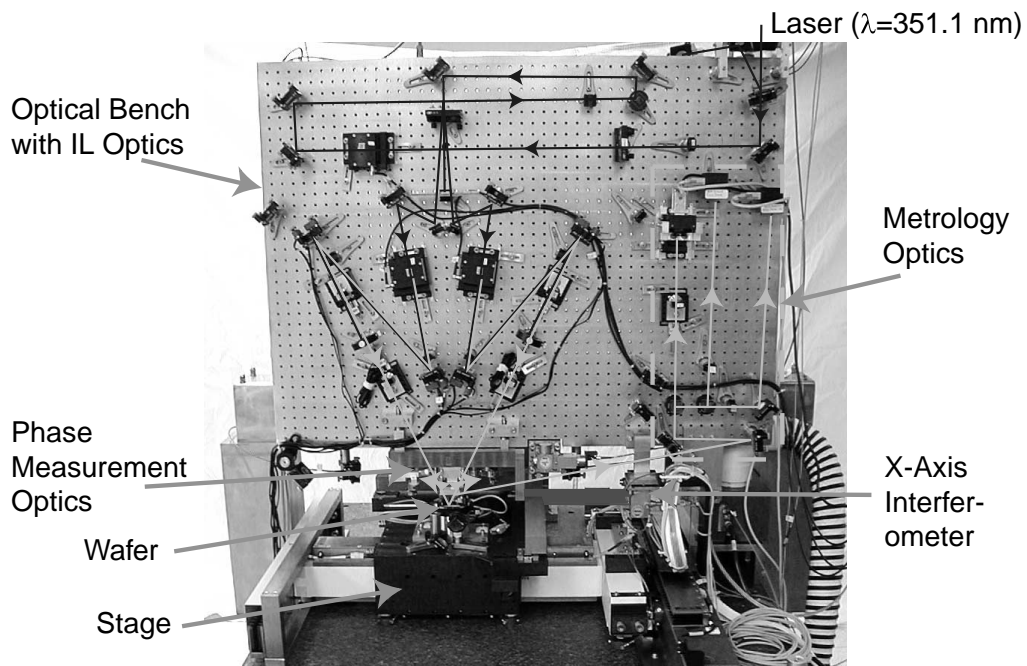
2. SYSTEM DESIGN

Figure 2 depicts the SBIL prototype currently under construction. Figure 3 shows its architecture. The system employs an XY air-bearing stage, four axes of column referencing heterodyne interferometry, refractometry, a grating length-scale reference, beam steering system, beam diagnostic and alignment system, wavefront metrology, acousto-optic fringe locking, and active and passive vibration isolation. Not shown is a Class 10 environmental enclosure that provides acoustic attenuation, as well as controls over temperature ($\pm 0.005\ \text{°K}$), relative humidity ($< \pm 0.8\%$), and pressure gradient ($< 15.5\ \text{Pa/m}$).

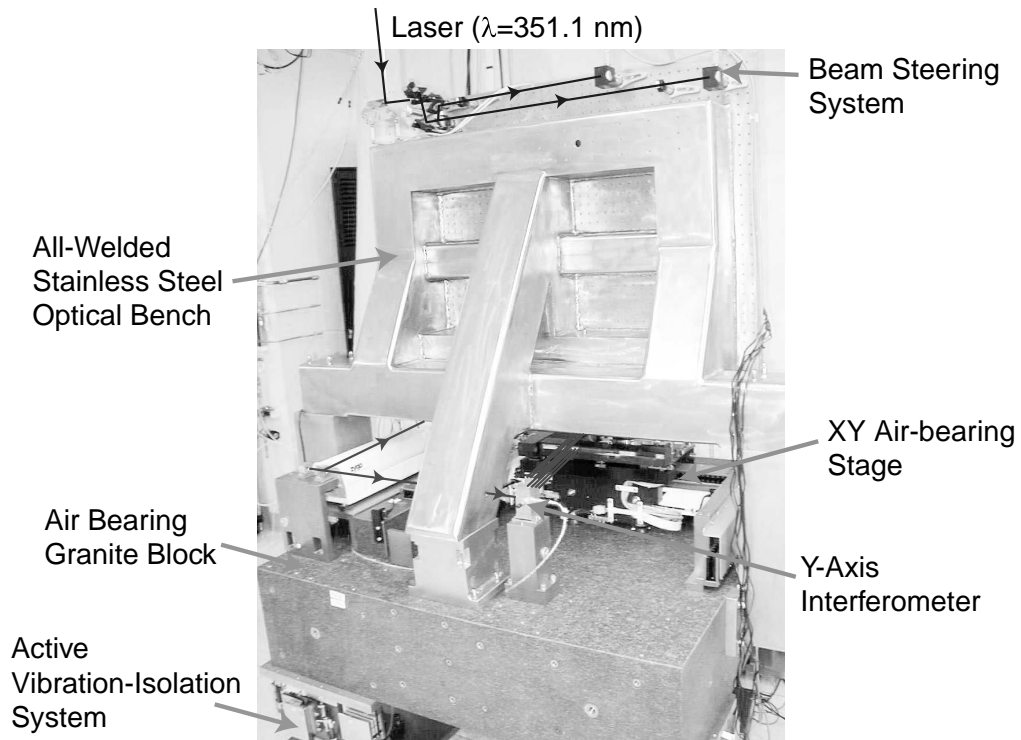
2.1. Displacement Measuring Interferometer

The most salient difference between traditional IL and SBIL is the step-and-scan feature provided by an XY air-bearing stage. The stage is controlled via displacement measuring interferometry (DMI). Large gratings are fabricated by scanning the substrate at a constant velocity underneath a small grating image (Fig. 1). At the end of each scan, the stage steps over by an integer number of grating periods and reverses direction for a new scan. Since the interfering beams have Gaussian intensity profiles, adjacent scans must be overlapped to ensure a uniform exposure dose.

Four column-referencing heterodyne interferometers, each with $0.3\ \text{nm}$ resolution, measure the stage x- and y-axis displacement and yaw. Error terms,^{9,10} such as the electronics error, polarization mixing error and mirror alignment error, all impact the accuracy of the DMI measurements, thence stage performance. Their



(a)



(b)

Figure 2. SBIL system, configured to write 400 nm period gratings. (a) Front view. (b) Rear view. Not shown is a Class 10 environmental enclosure.

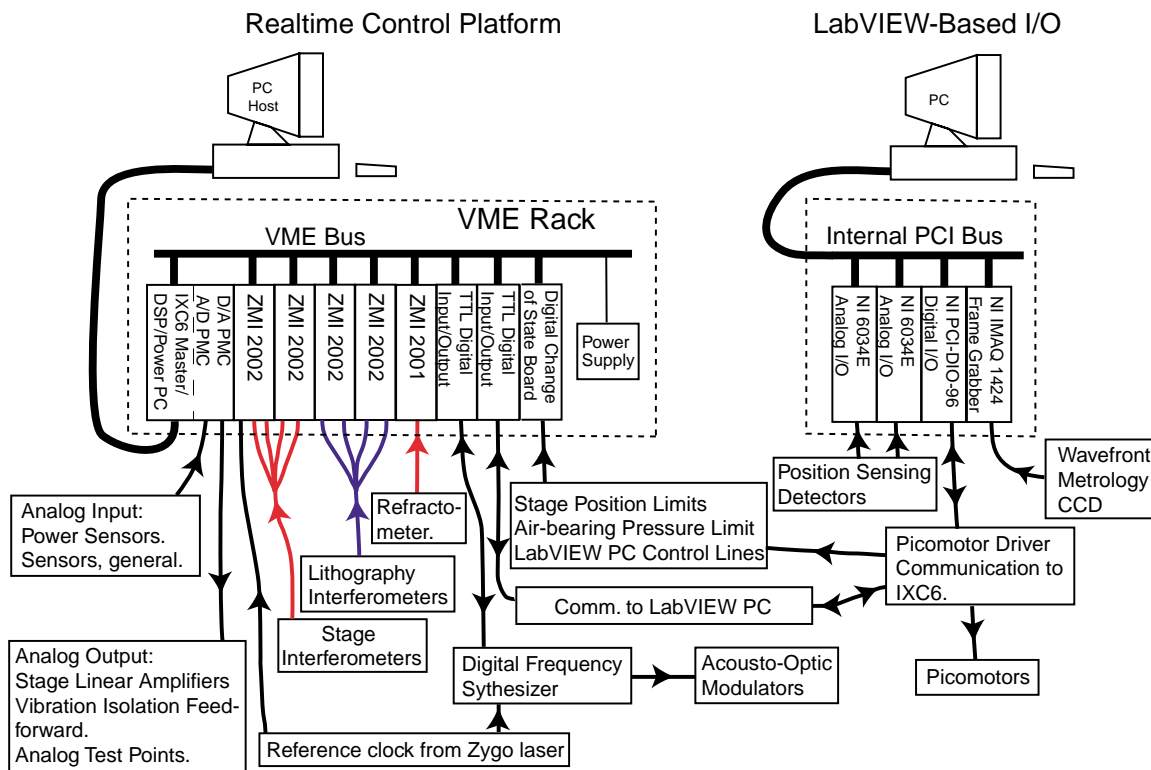


Figure 3. SBIL system architecture. The use of two separate platforms allows parallel software and hardware development.

effects combine into the so-called stage error (Fig. 4), which must be minimized during SBIL writing via real-time fringe-locking (Sec. 2.2). Furthermore, changes in the index of air and the vacuum wavelength of the DMI laser require an accurate way to scale the phase readings from our heterodyne electronics. A grating length-scale reference is included on the vacuum chuck to calibrate the wavelength of the stage interferometer.⁵ Our system is designed to read the phase of a grating that has nominally the same period as the one that we are set up to write.¹¹ Once calibrated, we use a refractometer to continuously monitor the wavelength change, thus allow real-time correction of the interferometer readout. To reject stage motion induced disturbances, we have implemented an active vibration isolation system with feed-forward control.

2.2. Lithography Interferometer

To reduce a major source of thermal and mechanical disturbances, and to allow multiple lithography tools to share a common laser, we have located our UV laser far (~ 10 m) from the SBIL system. A beam steering system¹² is constructed to stabilize the position and angle of the beam as it reaches the SBIL tool and forms the lithography interferometer.

The optical design of the interferometer incorporates means for spatial filtering and adjustment of intensity, polarization, wavefront curvature (Sec. 2.5), and spot size. A grating beamsplitter is used to separate the incoming laser into two beams that form the two arms of the interferometer⁵ (Fig. 1). The use of the grating provides a greater tolerance on the beam angular instability.¹² It also yields an achromatic configuration where the period of the interference fringes is insensitive to air index changes and vacuum wavelength variations of the UV laser.

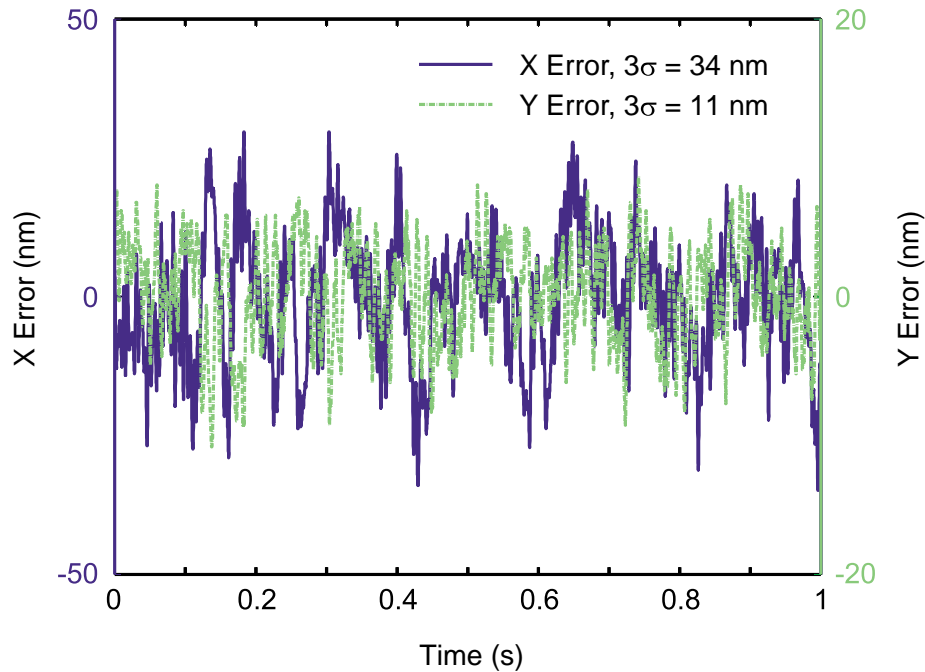


Figure 4. A sample stage error plot. The plot shows x and y position errors when the stage is nominally at rest. For this data set, the x-axis uses a column reference interferometer, whereas the y-axis uses an interferometer where the reference path is reflected within the interferometer head. By our choice, the stage x-axis is perpendicular to the interference fringes, and the y-axis parallel (Fig. 1). Column referencing enhances the accuracy for the critical x-axis because column drifts are incorporated as part of the stage error signal. However, column referencing diminishes the stage dynamic performance, as is clear by the three times greater error in x compared to y. Moreover, the rather large column tends to experience relatively high vibrational disturbances. Because the column dynamics require controllers with lower bandwidth, disturbance rejection is sacrificed. During SBIL operations, the x-axis stage error is fed back to a high bandwidth fringe locking system (Sec. 2.2).

During SBIL writing (Fig. 5(a)), lithography interferometer's phase error and the stage error are fed back to a high bandwidth heterodyne acousto-optic fringe locking system, which in real-time, locks the interference fringes to the moving substrate.¹¹ Performance of the fringe locking system is limited by the controller's bandwidth and inaccuracy in the fringe locking sensor signal due to air index variations and electronic inaccuracy. Our system's repeatability is established by reading the phase of a previously exposed grating (Fig. 5(b)). This measurement allows us to assess the repeatability of the stage displacement interferometer. Self-calibration procedures¹³ can then be implemented to correct systematic errors and translate repeatability into accuracy.

2.3. Substrate and Metrology Frame

Substrate and metrology frame errors refer to those from substrate distortion and the inability of the metrology reference surfaces, such as the stage interferometer mirrors and the column reference mirrors, to accurately measure the displacement between the fringes and the substrate.

Thermal and mechanical considerations have led to the design and installation of a rigid Zerodur metrology block, to which the x- and y-axis column reference mirrors (also made of Zerodur), and all critical phase measurement optics are attached (Fig. 2). Critical optic mounts, both on the metrology block and on the stage, have all been machined out of Invar, a low CTE material. A Super-Invar chuck is being readied as well, which can hold large substrates up to 300 mm in diameter with little distortion.

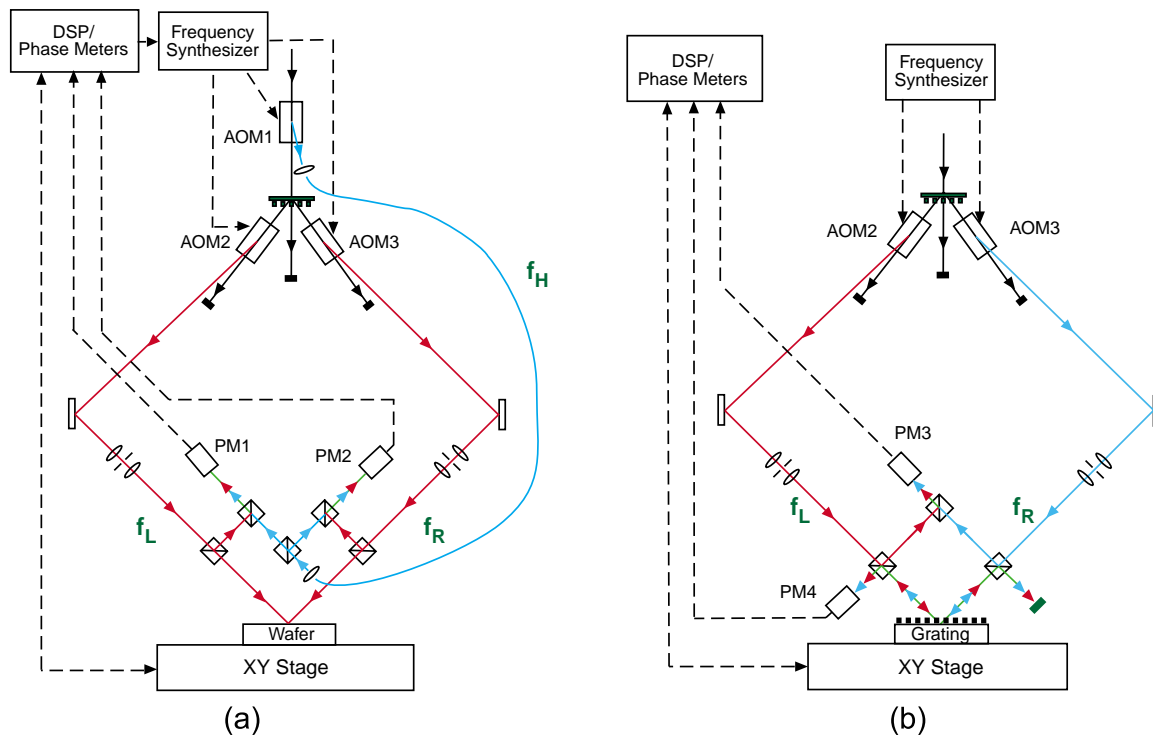


Figure 5. SBIL writing and reading modes. (a) Writing mode. By setting the frequencies to the acousto-optic modulators (AOM) and combining the appropriate diffracted beams, we generate two heterodyne signals at phase meters (PM) 1 and 2. A digital signal processor (DSP) then compares the signals and drives AOM2 to keep the phase difference between the two interferometer arms constant. (b) Grating reading mode. A grating is used in the so-called Littrow condition, where the 0-order reflected beam from one arm coincides with the -1-order back-diffracted beam from the other arm. Two heterodyne signals, PM3 and PM4, differ in the sense that PM4 contains the spot-averaged phase information from the grating.

2.4. Period Control and Beam Alignment

Equation 1 shows that the period of the grating image (p) will change if the wavelength of the laser (λ) or the angle of interference (θ) varies. For 1 nm of accumulated phase error across a 1 mm image radius, we must measure and control the grating period to one part per million.⁵ With a cube beamsplitter splitting the laser and forming the two arms of the lithography interferometer, the requirement on beam angle stability is severe. For example, for $p = 400$ nm, $\lambda = 351.1$ nm, and 1 nm phase error across a 1 mm beam radius, the allowed angle variation is only $0.5 \mu\text{rad}$. Fortunately, the application of a grating beamsplitter substantially alleviates the restriction on beam stability.¹²

We have developed a couple of simple interferometric techniques to measure the grating image period in-situ and with high accuracy.^{5,14} Figure 6 schematically demonstrates the one currently in use. An accurate knowledge of the period allows the correct stitching of adjacent scans and the proper feedback of stage error to the fringe locking controller.

Beam angle misalignment introduces additional phase errors due to substrate unflatness, and position misalignment ruins the fringe contrast. Therefore, both must be controlled. Beam alignment is also critical for SBIL wavefront metrology, fringe period metrology, and grating reading mode. To achieve beam angle and position alignment on the μrad and μm level, respectively, an automated beam alignment system has been built, based on the so-called iterative beam alignment principle.¹⁵ Repeatability experiments show that the system fulfills the alignment requirements for nanometer-level SBIL writing.

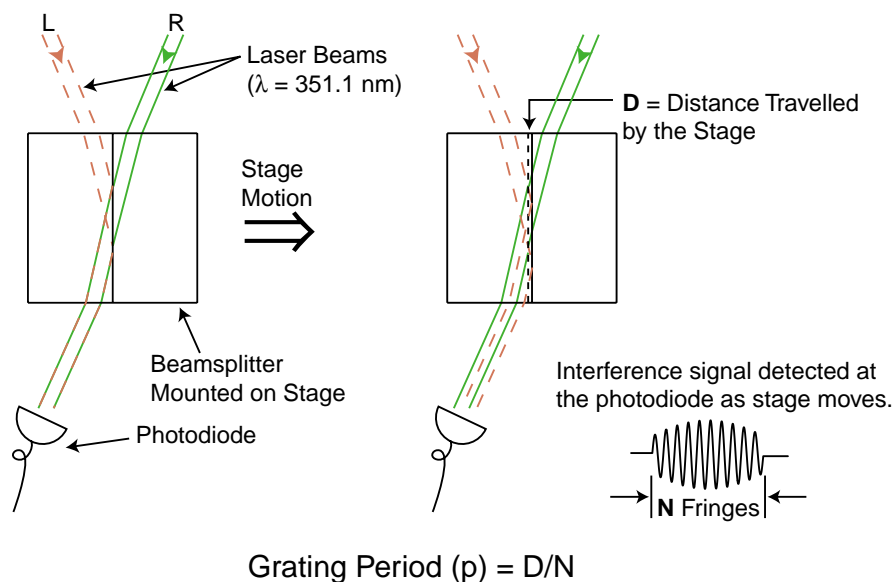


Figure 6. Period measurement via interferometry. The rectangular shape of the beamsplitter is specifically chosen so that the beamsplitter interface can be aligned parallel to the x-axis stage interferometer mirror (Fig. 1), which is perpendicular to the substrate. The alignment ensures the fringe perpendicularity to the substrate surface. Furthermore, it also ensures that the stage y-axis is the scan direction, thus no fringe-orientation measurement is necessary.

2.5. Wavefront Metrology

During SBIL, grating phase distortions along the scan direction can be averaged out. Overlap of adjacent scans provides even further averaging. Despite the averaging, excess phase distortions in the grating image is undesirable as it limits the system throughput and sacrifices the image contrast, thus must be minimized.

We have developed a quantitative method to map the phase distortions across a grating image, via phase shifting interferometry (PSI). The small beams used in SBIL are intrinsically Gaussian in nature.⁴ Lowest possible phase distortion is achieved when Gaussian beams interfere at their waists (Fig. 7(a)). If a metrology grating, used in its Littrow condition, is placed underneath the aerial image grating, Moiré fringes can be observed at a CCD camera due to the interference of the 0-order reflected and -1-order back-diffracted beams (Fig. 7(b)). These Moiré fringes arise from the phase difference between the image grating and the underlying metrology grating.¹⁶ If the metrology grating is well made and has an ideal linear phase, the Moiré fringes are a direct representation of the nonlinear phase distortions in the image grating. We can record a series of Moiré patterns by shifting the phase of one of the arms in the lithography interferometer through 2π . Out of the series, standard PSI algorithms can then be used to construct a phase distortion map (Fig. 8). By using the PSI data as feedback and adjusting the positions of the collimating lenses, we can modify the wavefront curvatures and minimize phase distortions in the image grating.

3. CONCLUSIONS

We have described the design for SBIL by addressing all five major subsystems: displacement measuring interferometer, lithography interferometer, substrate and metrology frame, period control and beam alignment, and wavefront metrology. For SBIL to perform with nanometer phase accuracy, all five subsystems have to function in coordination with little error. We have recently succeeded in using SBIL to pattern a cosmetically flawless grating over an entire 100 mm wafer. We are continuing our efforts to write and read gratings with nanometer-level phase accuracy.

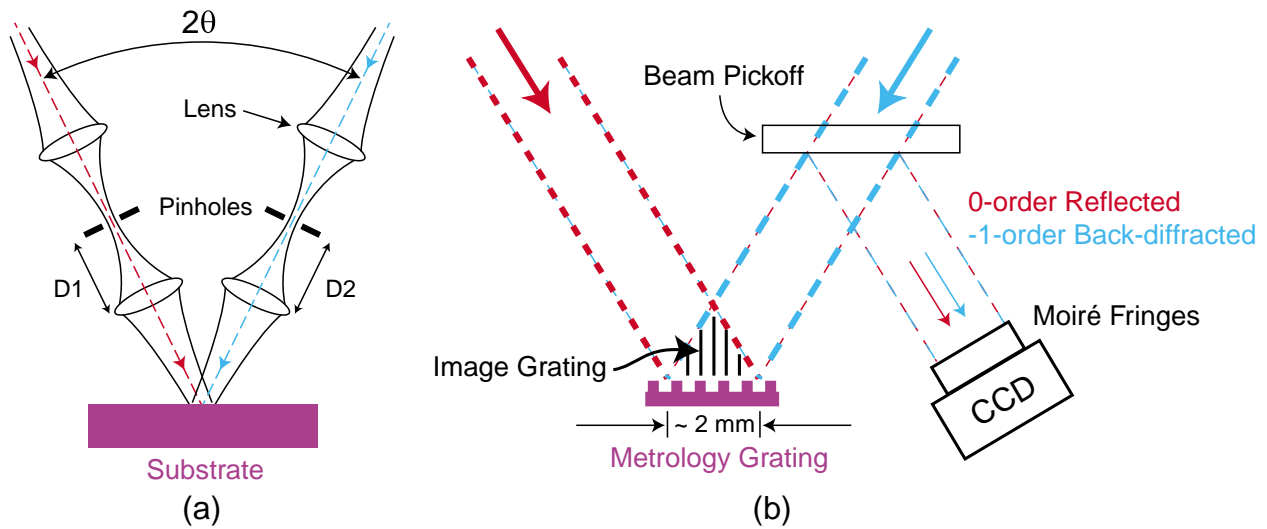


Figure 7. SBIL wavefront metrology. (a) The substrate plane phase distortion is a strong function of the distances D_1 and D_2 . (b) The metrology grating is a small patch of grating that can be cut out of a large grating made by traditional IL. Alternatively, it can be made via SBIL by overlapping many scans.

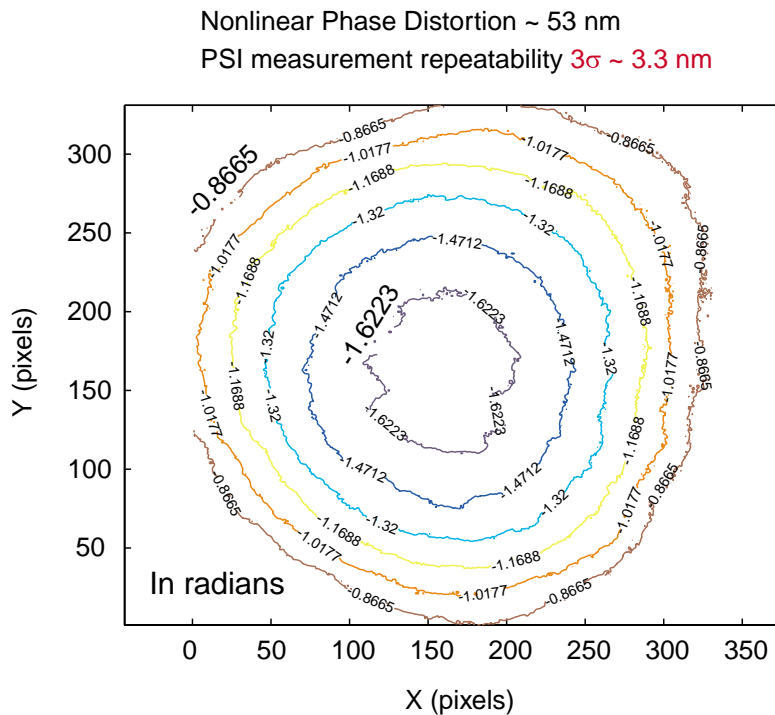


Figure 8. A sample phase distortion map. The metrology grating used has a period of $p \sim 400$ nm and is the central region of a larger grating produced by traditional IL. The Hariharan five-step algorithm¹⁷ is applied. The map shown is the average of 24 sets of PSI data, from which we can estimate a measurement repeatability of $3\sigma \sim 3.3$ nm. The x- and y-coordinates represent CCD camera pixels. This particular optical configuration yields a nonlinear phase distortion across the $1/e^2$ beam radius (~ 1 mm) of approximately 53 nm. A simulation based on a scalar Gaussian beam model¹⁸ predicts the same circular shape for the distortion map.

ACKNOWLEDGMENTS

The authors gratefully acknowledge the outstanding technical assistance of James Carter, Robert Fleming and Edward Murphy. Student, staff, and facility support from the MIT Space Nanotechnology Laboratory and the MIT NanoStructures Laboratory are also appreciated. This work was supported by DARPA under Grant No. DAAG55-98-1-0130 and NASA under Grant No. NAG5-5271.

REFERENCES

1. J. Ferrera, *Nanometer-Scale Placement in Electron-Beam Lithography*. PhD dissertation, Massachusetts Institute of Technology, Department of Electrical Engineering and Computer Science, June 2000.
2. K. Hibinio and Z. Hegedus, "Hyperbolic holographic gratings: analysis and interferometric tests," *Applied Optics* **33**, pp. 2553–2559, May 1994.
3. J. Ferrera, M. Schattenburg, and H. Smith, "Analysis of distortion in interferometric lithography," *J. Vac. Sci. Technol. B* **14**, pp. 4009–4013, Nov.-Dec. 1996.
4. C. G. Chen, *Microcomb Fabrication for High Accuracy Foil X-ray Telescope Assembly and Vector Gaussian Beam Modeling*. Master's thesis, Massachusetts Institute of Technology, Department of Electrical Engineering and Computer Science, June 2000.
5. C. G. Chen, P. T. Konkola, R. K. Heilmann, G. S. Pati, and M. L. Schattenburg, "Image metrology and system controls for scanning beam interference lithography," *J. Vac. Sci. Technol. B* **19**, pp. 2335–2341, Nov.-Dec. 2001.
6. M. L. Schattenburg, C. Chen, P. N. Everett, J. Ferrera, P. Konkola, and H. I. Smith, "Sub-100nm metrology using interferometrically produced fiducials," *J. Vac. Sci. Technol. B* **17**, pp. 2692–2697, Nov.-Dec. 1999.
7. P. T. Konkola, C. G. Chen, R. K. Heilmann, G. S. Pati, and M. L. Schattenburg, "Scanning beam interference lithography," *Proceedings of ASPE*, Nov. 2001.
8. M. L. Schattenburg and H. I. Smith, "The critical role of metrology in nanotechnology," *Proc. SPIE* **4608**, pp. 116–124, 2001.
9. N. Bobroff, "Recent advances in displacement measuring interferometry," *Meas. Sci. Technol.* **4**, pp. 907–926, 1993.
10. F. C. Demarest, "High-resolution, high-speed, low data age uncertainty, heterodyne displacement measuring interferometer electronics," *Meas. Sci. Technol.* **9**, pp. 1024–1030, 1998.
11. R. K. Heilmann, P. T. Konkola, C. G. Chen, G. S. Pati, and M. L. Schattenburg, "Digital heterodyne interference fringe control system," *J. Vac. Sci. Technol. B* **19**, pp. 2342–2346, Nov.-Dec. 2001.
12. P. T. Konkola, C. G. Chen, R. K. Heilmann, and M. L. Schattenburg, "Beam steering system and spatial filtering applied to interference lithography," *J. Vac. Sci. Technol. B* **18**, pp. 3282–3286, Nov.-Dec. 2000.
13. C. J. Evans, R. J. Hocken, and W. T. Estler, "Self-calibration: reversal, redundancy, error separation, and "absolute testing"," *CIRP Annals* **45**(2), pp. 617–634, 1996.
14. C. Joo, C. G. Chen, P. T. Konkola, R. K. Heilmann, G. S. Pati, and M. L. Schattenburg, "Nanometer-accurate fringe metrology using a Fresnel zone plate," to be published in *J. Vac. Sci. Technol. B*, Nov.-Dec. 2002.
15. C. G. Chen, R. K. Heilmann, C. Joo, P. T. Konkola, G. S. Pati, and M. L. Schattenburg, "Beam alignment for scanning beam interference lithography," to be published in *J. Vac. Sci. Technol. B*, Nov.-Dec. 2002.
16. D. Malacara, Ed., *Optical Shop Testing*, Wiley, 2nd ed., 1992.
17. P. Hariharan, B. F. Oreb, and T. Eiju, "Digital phase-shifting interferometry: A simple error-compensating phase calculation algorithm," *Applied Optics* **26**, p. 2504ff, 1987.
18. C. G. Chen, P. T. Konkola, J. Ferrera, R. K. Heilmann, and M. L. Schattenburg, "Analyses of vector Gaussian beam propagation and the validity of paraxial and spherical approximations," *J. Opt. Soc. Am. A* **19**(2), pp. 404–412, 2002.